GEOG 321 - Reading Package Lecture 13

RADIATION BUDGET OF SNOW AND ICE

Radiatively, snow and ice surfaces are very much more complex than the surfaces we have considered previously. One of the most important differences is that snow and ice both allow some transmission of short-wave radiation. This means that the shortwave radiation incident at any depth can be transmitted, reflected or absorbed according to equation (1.6):

$$\Psi_\lambda + \alpha\lambda + \zeta_\lambda = 1 \qquad \star \quad (8.1)$$

and that radiation absorption occurs within a volume rather than at a plane. This results in a flux density convergence because the shortwave radiation incident at the surface ($K_{\downarrow 0}$) is greater than that found at any depth z below.

Beer's Law. The decay of the flux with distance into the snow or ice follows an exponential curve so that the quantity of shortwave radiation reaching any depth z is given by:

$$K_{\downarrow z} = K_{\downarrow 0}\, e^{-k\, z} \qquad \star \quad (8.2)$$

where $K_{\downarrow z}$ shortwave radiation incident at depth z, e base of natural logarithms, k extinction coefficient (m^{-1}). Equation 8.2 is known as *Beer's Law* and strictly is applicable only to the transmission of individual wavelengths in a homogeneous medium, but it has been used with success for fairly wide wave-bands (especially the shortwave) in meteorological applications. The extinction coefficient k depends on the nature of the transmitting medium, and the wavelength of the radiation. It is greater for snow than for ice and hence the depth of penetration is greater in ice. The depth of shortwave penetration can be as great as 1 m in snow, and 10 m in ice. The exponential form of the depletion means that absorption is greatest near the surface and tails off at lower depths.

The internal transmission of radiation through snow and ice gives problems in formulating the surface balance and in observation. For example, measurements of reflected shortwave from an instrument mounted above the surface include both surface and sub-surface reflection. The albedo calculated from such measurements is therefore a volume not a surface value. Consider also the practical problem of an instrument buried within snow or ice to measure the temperature, or heat flow at depth. Such a body is likely to absorb transmitted radiation causing it to warm up and become an anomalous thermal feature. It therefore records its own response and not that of the surrounding environment.

Reflectance. One of the most important characteristics of snow and ice is their high albedo (α, see also Reading Package Lecture 6). Their rejection of such a large proportion of $K_\downarrow$ is of primary importance in their overall low energy status. The introduction of even a thin snow cover over the landscape has dramatic effects. In a matter of a few hours a natural landscape can experience a change in albedo from approximately 0.25 to perhaps 0.80. Thereafter α declines as the snow pack ages (becomes compacted, and soiled), but with a fresh snowfall it rapidly increases again. The albedo of most natural surfaces exhibits a diurnal variation with high values in the early morning and evening and a minimum near midday. Indeed when α is plotted on a graph against the solar zenith Z (or altitude β) angle a clear exponential relation emerges. Such behaviour suggests specular (mirror-like) rather than diffuse reflection. This is further supported by the facts that the curve is best displayed on days when direct beam (S) rather than diffuse radiation (D) is prevalent, and over relatively smooth rather than rough surfaces.

In the case of ice and snow this variation may also be due to physical changes in the state of the surface, especially if conditions are conducive to surface melting. In the early morning and evening the surface is frozen and this, combined with the high zenith angle Z of the Sun, gives a relatively high albedo α. In the afternoon even a thin film of meltwater on the surface serves to reduce α to a value closer to that of water. It should also be noted that the spectral reflectivity α_λ of snow varies with wavelength, being highest for the shortest wavelengths (ultra-violet and visible blue) and decreasing to quite low values in the near infrared. This is almost the reverse of the case for soil and vegetation surfaces.
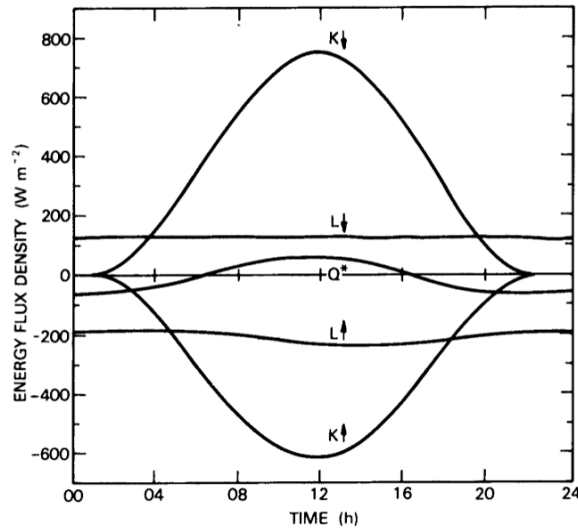
Figure 1: Variation of the radiation budget components over snow at Mizuho Station, Antarctica (70°S), on 13 November 1979 (after Yamanouchi et al., 1981).

The wavelength dependence of the albedo of snow helps to explain the ease with which human skin becomes sunburnt, especially on sunny days on snow covered mountains. Human skin is very sensitive to ultra-violet (UV) radiation, with peak sensitivity at about $0.3\,\mu\mathrm{m}$. The potential for sunburn stretches from 0.295 to $0.330\,\mu\mathrm{m}$. The lower limit is governed by the almost total absorption of these wavelengths by ozone in the high atmosphere (Reading Package Lectures 3-4, Figure 5, Panel b). With a fresh snow cover the receipt of potentially burning ultra-violet radiation by exposed skin is almost doubled, because in addition to that received from the incoming beam there is a very significant proportion received after surface reflection (due to the high value of α_λ at these short wavelengths). The upward flux is responsible for sunburn on earlobes, throat and within nostrils, areas which are sensitive and normally in shade.

Longwave radiation. In the longwave portion of the spectrum, ice and snow (and especially fresh snow) are almost full radiators. However, although their emissivity ε is high the absolute magnitude of $L_\uparrow$ is usually relatively small because the surface temperature T_0 is low. One helpful simplification occurs if the surface is melting. Then T_0 is set at $0°C$ (273.2 K) and if it is assumed that $\varepsilon_{\mathrm{snow}} = 1.0$ the value of $L_\uparrow$ is constant at $316\,\mathrm{W\,m^{-2}}$ (Stefan-Boltzmann law). Since clouds are also close to being full radiators the net longwave exchange (L^*) between a fresh snowpack and a complete

overcast is simply a function of their respective temperatures:

$$L^* = L_\uparrow - L_\uparrow \approx \sigma(T_c^4 - T_0^4) \qquad (8.3)$$

where T_c - cloud-base temperature). Should the cloud-base be warmer than the snow surface there will actually be a positive L^* budget at the snow surface. With clear skies L^* is almost always negative, as is true of most other surfaces.

Net allwave radiation. In general it may be said that the daytime net radiation surplus (Q^*) of snow and ice is small by comparison with most other natural surfaces. This is directly attributable to the high surface albedo. In the case of the Antarctic early summer budget shown in Figure 1 the surface albedo is 0.80. This results in so little shortwave radiation absorption that when it is combined with a net longwave loss, that is quite similar to other environments, the midday net allwave radiation is less than 10% of the incoming solar radiation $K_\downarrow$. Indeed even though the daylength at this high latitude is about 21 h, the total daily net radiation is negative (approximately $-1.0\,\mathrm{MJ\,m^{-2}\,d^{-1}}$).

ENERGY BALANCE OF SNOW AND ICE

The energy balance of snow is complicated not only by the penetration of shortwave radiation into the pack but also by internal water movement, and phase changes. Water movement inside a snowpack may be due to the percolation of rainfall, or of meltwater. If the water temperature is significantly different to that of deeper layers it will involve heat as well as mass transport. In the case of rain percolation, this represents an additional heat source for the pack; in the case of meltwater it merely involves an internal re-distribution of heat. Phase changes of water within the pack (e.g. freezing, melting, sublimation, evaporation or condensation) involve energy uptake or release at that location. For example, if rainwater percolating through the pack freezes it will release latent heat of fusion which is available to warm the surrounding snow.

All of these features make it difficult to formulate an accurate surface energy or water balance for snow or ice. A better approach is to consider a volume balance and to treat all fluxes as equivalent flows through the sides of the volume. If we ignore horizontal energy transfers and define the volume as extending from the surface to a depth where there is no significant vertical heat flux (Figure 2) then the energy balance equation becomes:

$$Q^* = Q_H + Q_E + \Delta Q_S + \Delta Q_M \qquad \star \quad (8.4)$$
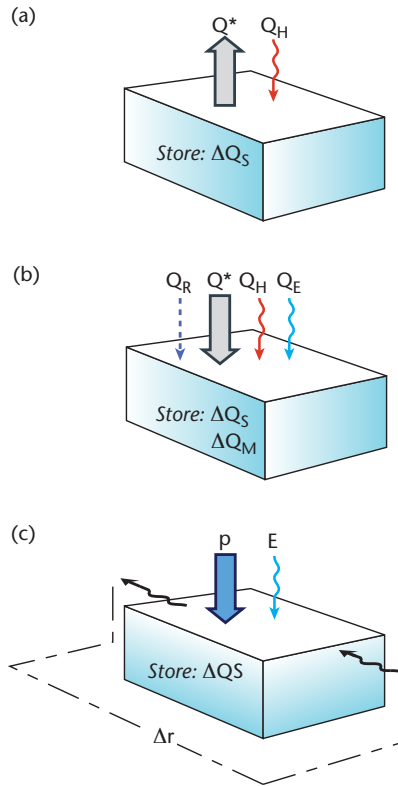
(a)

(b)

(c)

Figure 2: Schematic depiction of the fluxes involved in the (a, b) energy and (c) water balances of a snowpack volume. The energy balances are for (a) a 'cold' or frozen pack and, (b) a 'wet' or melting pack.

The net heat storage term (ΔQ_S) then represents the convergence or divergence of sensible heat fluxes within the volume. This term includes internal energy gains or losses due to variations of radiation, and heat conduction. Phase changes of water in the snow or ice volume are accounted for by ΔQ_M which is the latent heat storage change due to melting or freezing. Equation 8.6 can also include a soil heat flux density (Q_G) if the snow layer is thin and there is significant heat exchange across the base of the pack.

The energy balance of a snow volume depends upon whether it is a 'cold' (less than $0°C$) or a 'wet' ($0°C$, often isothermal) pack.

'Cold' snowpacks. Let us consider the case of a 'cold' snowpack typical of high latitudes in winter with little or no solar input. Under these conditions Q_E and ΔQ_M are likely to be negligible because there is no liquid water for evaporation, little atmospheric vapour for condensation or sublimation, and both the precipitation

and the contents of the snowpack all remain in the solid phase. Similarly heat conduction within the snow will be very small because of the very low conductivity of snow and the lack of any solar heating, so ΔQ_S and Q_G are also negligible. As a result the energy balance (Figure 2a) is basically between a net radiative sink (Q^*) and a convective sensible heat source (Q_H). The radiation budget is negative because it is dominated by longwave exchanges, and the outgoing flux ($L_\uparrow$) is readily able to escape through the atmospheric 'window' (if there is no cloud) because of the lack of atmospheric water vapour and other absorbing agents (e.g. pollutants). A radiation inversion exists because of the surface cooling, hence any mixing acts to transfer heat from the atmosphere to the snow surface.

It is also possible to find 'cold' snowpacks where Q^* and Q_E are significant energy sources for the pack. For example, on a summer day the snow cover on a high latitude ice cap or glacier may be in receipt of considerable amounts of radiation. This results in radiation absorption in the upper layers and generates a heating wave which is transmitted downwards by conduction, so that ΔQ_S becomes significant over short periods. Taken overall, however, these gains are not sufficient to raise temperatures above $0°C$. In cloudy, moist areas it is possible that a 'cold' snowpack can receive energy via Q_E. With the surface temperature below $0°C$ vapour may sublimate directly onto the surface as hoar frost or rime. In these circumstances we can write:

$$Q_E = L_s E \qquad (8.5)$$

where $L_s E$ the latent heat released due to the sublimation of vapour onto the surface at the rate E. On mountain tops where the water distribution within the cloud is essentially uniform with height the amount of rime accretion is related to the rate of vapour supply. The rate of delivery is a function of the variation of wind speed with height. Therefore with a steady wind the ice loading on an object usually increases with height and is greater in the windward direction. A careful survey of rime accretion on trees, poles, etc. following such events can be very helpful in discovering local airflow patterns across the landscape and around obstacles.

'Wet' snowpacks. A wet snowpack during the melt period the surface temperature will be held very close to $0°C$ but the air temperature may be above freezing. Precipitation may then be as rain and the energy balance (Figure 2b) becomes:

$$Q^* + Q_R = Q_H + Q_E + \Delta Q_S + \Delta Q_M \quad \star \quad (8.6)$$
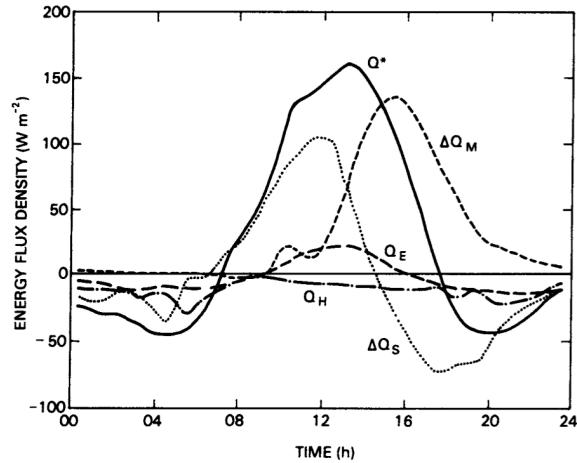
Figure 3: Energy balance components for a melting snow cover at Bad Lake, Saskatchewan (51°N) on 10 April 1974 (modified after Granger and Male, 1978).

where Q_R heat supplied by rain if its temperature is greater than that of the snow. In some mid-latitude locations Q_R can be a significant energy source for melt, especially where the area is open to storms originating over warm oceans. Some melting snowpacks are isothermal throughout a deep layer, others have a temperature stratification similar to that in a soil. In the former, by definition, heat transfer is zero, but in the latter percolating rain and meltwater, and its subsequent re-freezing, are primary means of heat transfer (i.e. conduction is small). During active melting both radiation (Q^*) and convection ($Q_H + Q_E$) act as energy sources (Figure 2b) to support the change of phase (ice to water). The temperature of the snow changes very little in this process; therefore the large change of energy storage is due to latent rather than sensible heat uptake, i.e. ΔQ_M rather than ΔQ_S.

The role of Q_E in the case of 'wet' snow is interesting. The surface vapour pressure of a melting ice or snow surface is of course the saturation value (e^*) at $0°C$ which equals 611 Pa (See Oke, 1987, Table A3.2, p. 394). In absolute terms this is a low value and it is very common to find the warmer air above the surface has a greater vapour pressure. In that case an air-to-surface vapour pressure gradient exists, so that any turbulence contributes a downwards flux of moisture, and condensation on the surface. Since at $0°C$ the latent heat of vaporization (L_v) released upon condensation is 7.5 times larger than the latent heat of fusion (L_f) required for melting water, for every 1 g of water condensed sufficient energy is supplied to melt a further 7.5 g. Under these conditions Q_E is an important energy source. Of course should the air be drier than 611 Pa the vapour gradient would be the reverse, evaporation would occur

and Q_E would become an energy sink in the balance.

An example of the energy balance of a melting snow cover from the Canadian Prairies in Spring is given in Figure 3. The primary source of energy for the melt in this case is the net radiation. At midday Q^* is only about $150 \mathrm{W\,m^{-2}}$ because the snow albedo was about 0.65. There is a small input of sensible heat by turbulent transfer throughout the day. This is because the airmass was slightly warmer than the snow surface. The advection of warm air by weather systems, or from upwind bare surfaces, can greatly enhance the role of this source in melting. On other occasions, when the air is cooler than the surface, Q_H is a small sink for heat together with Q_E. In Figure 3 heat conduction into the soil is not large enough to warrant inclusion.

Prior to noon the heat input to the pack is almost entirely put into storage, ΔQ_S. This is used to raise the snow temperature from its overnight value to the freezing point and then to change the proportions of ice and water in the pack. The melt peaks in the afternoon period and then declines as the pack cools again. The decline is retarded somewhat by the release of latent heat of fusion (L_f) as the upper layers re-freeze. The direct association between the energy and water balances of the snow cover are explicit here. In fact the values of ΔQ_M were calculated by measuring the meltwater runoff rate per unit area, Δr:

$$\Delta Q_M = L_f \, \Delta r \qquad (8.7)$$

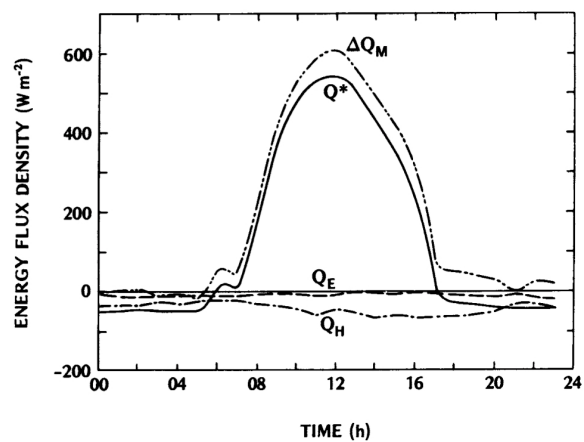if Δr has the units kg m^{-2} s^{-1}.

Figure 4: Energy balance components for the surface of a melting glacier at Peyto Glacier, Alberta (51°N) on 29 August 1971 (data after Munro, 1975).

If Δr is measured in the more familiar hydrologic units

4

(mm h^{-1} or mm day^{-1}):

$$\frac{\Delta r}{\Delta t} = \frac{\Delta Q_M}{\rho_w L_f} \tag{8.8}$$

An error in the timing of ΔQ_M is introduced in this procedure because of the lag between the melt process and the emergence of meltwater runoff at the base of the pack.

In the case study shown in Figure 3 radiation was responsible for about 68% of the melt and convection $(Q_H + Q_E)$ for about 31%. Although small on an hourly basis the role of Q_H is significant over a complete day because, unlike Q^*, it did not change sign.

Figure 4 gives the results of an energy balance study over a mid-latitude alpine glacier during an almost cloudless day in the summer melt period. The surface of the glacier is soiled with morainic materials, therefore the albedo is relatively low and the net radiation is relatively large. Throughout the period both the air temperature and vapour pressure gradients remained inverted. Thus the surface was continually in receipt of sensible and latent heat from the atmosphere. At night the combined convective transfer $(Q_H + Q_E)$ was sufficient to allow the net radiant emission to be offset or surpassed and therefore was able to support a small amount of ice melt. By day the convective gain supplemented that from radiation and permitted an augmented rate of melting (ΔQ_M). Changes of temperature, and therefore ΔQ_S, were negligible. Over the complete day the convective supply provided 29% of the total energy used in the melt (23% Q_H, 6% Q_E), and the remaining 71% came from net radiation absorption. This ranking of heat sources during the melt season agrees with many glacier energy balance studies. It also applies to snow melt over other open surfaces (e.g. tundra and prairie sites), but in forested areas the trees are efficient absorbers of shortwave radiation and act as sources of sensible heat and longwave radiation for the surrounding snow.

Water balance. The water balance of a snow or ice volume with its upper side at the snow or ice/air interface, and with its lower side at the depth of negligible water percolation (Figure 2c) is given by:

$$\Delta S = pE + \Delta r \tag{8.9}$$

Hence the net change of mass storage (ΔS) is due to the precipitation input (snow or rainfall); the net turbulent exchange with the atmosphere (input as condensation and sublimation, or output as evaporation and sublimation); and the net surface and sub-surface horizontal exchange (surface snow drifting and meltwater flow or sub-surface meltwater throughflow). In the simple case, ΔS can be related to snow depth so that it increases after a storm, and decreases as a result of melting. However, depth changes can also be due to an increase in snow density (i.e. a decrease in volume with no change in mass). Density changes are a feature of snow ageing and could be due to simple compaction, re-freezing and metamorphism of ice crystals. Therefore, rather than snow depth it is more pertinent to measure ΔS in terms of an equivalent depth of water (i.e. the depth of water obtained by melting unit volume of the ice or snow, or weighing a snow core of known cross-sectional area). As mentioned this conversion will vary with density but as an approximate rule-of-thumb 100 mm of snow is equivalent to 10 mm of water. It is then an easy task to convert the water equivalent to the energy required to evaporate or melt this depth of water using the appropriate latent heat.

For the case shown in Figure 3, the latent heat flux (Q_E) is equivalent to an evaporation (E) of 0.03 mm of water over the day. The water equivalent of the melt was almost 9 mm, so with the snow density of 288 kg m^{-3} this should have produced a snow lowering of about 30 mm. For the Peyto Glacier (Figure 4) the corresponding melt is 48 mm and this would have been slightly offset by a 0.4 mm addition of mass due to E.

SNOW CLIMATES

The sub-surface temperature profiles typical of a deep snow pack are unlike those of soil, because of the occurrence of a temperature maximum just beneath the surface. This feature is a result of the fact that by day radiative heat transfer dominates over heat conduction in the upper 0.5 m of snow, and the upper 5 m in ice, and also because shortwave radiation is transmitted very much more readily than longwave radiation in these media. If we ignore conduction the pattern of energy gain/loss by the upper layers of the snow pack is given by the vertical profile of Q^* as illustrated in Figure 5. The radiative input (both short- and longwave) to the pack from above is absorbed in general accord with Beer's Law (equation 8.2). The longwave portion is relatively quickly absorbed, but shortwave penetrates to much greater depths. The radiative loss consists of shortwave reflection, and that longwave emission able to escape to the atmosphere. The strong absorptivity of snow in the infrared only allows this loss to occur from a thin surface layer.
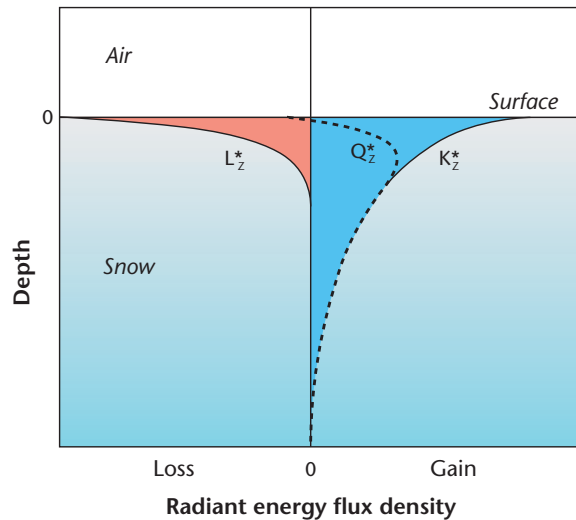
Figure 8: Conceptual distribution of shortwave and longwave radiation in a snow pack.

Therefore the net radiation at any depth (Q_z^*, the difference between these gains and losses) shows a maximum absorption just below the surface during the day. This level, and not the snow surface, is the site of maximum heating, and therefore has the highest temperature. If Q^* dominates the melt at a site it is therefore most effective below the surface and this accounts for the 'loose' or 'hollow' character of the surface of a melting snowpack. At night with only longwave radiative exchange the active surface is at, or very near, the actual surface. The lowest nocturnal temperatures occur at the snow surface, and the daytime sub-surface temperature maximum migrates downward by conduction.

Figure 6: Melthole caused by a stone absorbing shortwave radiation in the snow pack.

As was mentioned previously buried instruments may become anomalously warm (compared with the snow or ice at the same depth) because their opacity and low albedo dictate that they preferentially absorb shortwave radiation reaching that depth. All buried objects will act in this way, and some of the most common include stones, twigs, leaves, dirt layers, and the bases of trees or fences. The radiant heating of these objects may be sufficient to melt the overlying or surrounding snow (Figure 6). This gives rise to micro-relief features such as melt-holes corresponding to the shape of the object. If the snow cover is less than 0.15 m deep, absorption by the underlying surface (e.g. soil) may become significant in helping to melt the layer from below.

The very low conductivity and diffusivity of snow (especially when fresh) makes it an effective insulating cover for the ground beneath. This is especially true at night when radiative exchange is concentrated in the surface layer of the snow. Then as little as 0.1 m of fresh snow will insulate the ground from snow surface temperature changes, and thereby help to conserve soil heat. In many locations farmers are keen to retain a deep snow cover over their land during the winter and early spring for three reasons. First, the snow minimizes frost penetration and thus hastens spring warm- up ready for seed germination. Second, snow meltwater may be a significant source of soil moisture. Third, the snow cover may provide thermal protection for early seedlings. Plants within snow are in a conservative if cool environment, but if portions protrude above the surface they are open both to a wider range of temperature fluctuations, and to abrasion by blowing snow and ice pellets. A harmful situation occurs when the root zone is frozen but the exposed shoots are warmed by the Sun. If transpiration occurs the plant is unable to replace plant water losses via its root system and it dies from dessication.

At night the poor diffusivity of snow results in fast surface cooling and the development of intense inversions based at the surface. Over snow- covered surfaces at high latitudes winter radiative cooling is almost continuous which leads to semi-permanent inversion structures. In these circumstances it is not uncommon to encounter a temperature increase of 20C in the first 20 m above the surface. These inversions are not usually destroyed by convective heating generated at the surface. Their breakdown is due to mechanical mixing induced by an increase in wind speed. Any increase in turbulence results in an enhanced transfer of sensible heat towards the surface from the relatively warmer air above. This accounts for areas of relative warmth observed to occur downwind of isolated obstacles, or zones of increased roughness such as clumps of vegetation, buildings, etc.

In absolute terms the amount of water vapour in air over extensive snow-covered surfaces is very small. This is due to the lack of local moisture sources (if the surface temperature is below freezing), and to the low saturation vapour pressure of cool or cold air. However, even if the surface is melting the surface cannot exceed a saturation vapour pressure of 611 Pa, therefore a strong evaporative gradient cannot develop unless the air is exceptionally dry.

Avalanches form on slopes when stresses in the snow overcome its strength, resulting in failure. The strength of snow depends upon its temperature and density. Temperature is especially critical: shear strength decreases as temperatures rise towards 0°C. Stresses are increased by overloading caused by additional falls of snow or rain or the weight of a skier. Failure commonly occurs at breaks of slope or down-slope of protrusions (rocks, trees, etc.). Weakness at depth can cause large slabs to slide downhill.

8.1 LIQUID WATER SURFACES

The thermal and dynamic properties of water bodies (oceans, seas, lakes, etc.) makes them very important stores and transporters of energy and mass. The exchanges occurring at the air/water interface are, however, complicated by the fact that water is a fluid. This means that heat transfer within water is possible not only by conduction and radiation, but also by convection and advection. As in the atmosphere these modes of transfer greatly facilitate heat transport and mixing, and thereby allow heat gains or losses to be spread throughout a large volume. Although water is not compressible like air, it can be deformed, giving surface waves.

Radiation budget of lakes and oceans. Shortwave radiation can be transmitted within water, and its variation with depth is well approximated by Beers law (equation 8.2), with the extinction coefficient dependent upon both the nature of the water and the wavelength of the radiation. It depends upon the chemical make-up, plankton growth, and turbidity (amount of suspended material) of the water, and increases with wavelength towards the infrared. This spectral dependence was noted in the case of snow and ice and is in accord with the absorptivity spectrum of water vapour and cloud (see Figure 5 in Reading Package Lecture 4-5).

Obviously the more absorbing substances there are in the water the greater is the extinction coefficient, and the

less the penetration. In most water bodies shortwave radiation is restricted to the uppermost 10 m, but in some very clear tropical waters it has been observed to reach 700 to 1000 m. The different colours of lakes (especially blue and green combinations) are a result of different values of the extinction coefficient in the visible portion of the electromagnetic spectrum, which in turn are a result of differences in lake water composition.

The albedo (α) of a water surface, like that of snow, is not constant. In particular it depends upon the angle at which the direct beam (S) strikes the surface. With cloudless skies and the Sun at least 30° above the horizon, water is one of the most effective absorbing surfaces (α in the range 0.03 to 0.10), but at lower solar altitudes its reflectivity increases sharply. When the Sun is close to the horizon near sunrise and sunset the reflection is mirror-like, and this accounts for the dazzling effect at these times. Under cloudy skies the diffuse solar radiation (D) forms a larger proportion of the incoming solar radiation ($K_\downarrow$), and the effect of solar altitude is considerably dampened (Figure 7). The altitude dependence is also modified by the roughness of the water surface. With a roughened surface (waves) and high solar altitudes there is a greater probability that the incident beam will hit a sloping rather than a horizontal surface, thereby tending to increase α; whereas at low altitudes instead of grazing the surface the beam is likely to encounter a wave slope at a local angle which is more conducive to absorption, thereby decreasing α in comparison with smooth water. In all cases the albedo includes reflection from within the water as well as from the surface.
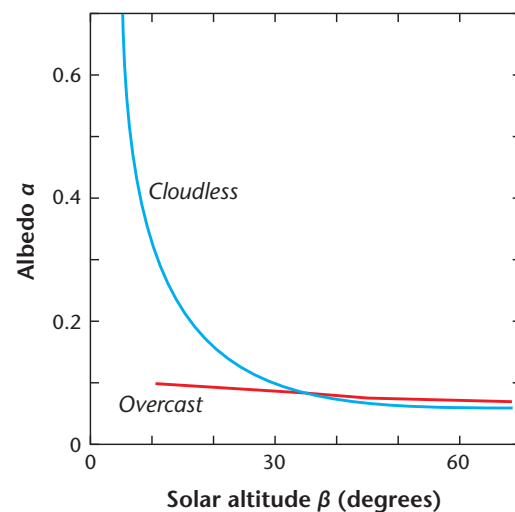

Figure 7: Relation between solar altitude β and the albedo α of lake water for clear and cloudy days over Lake Ontario (after Nunez et al., 1972).
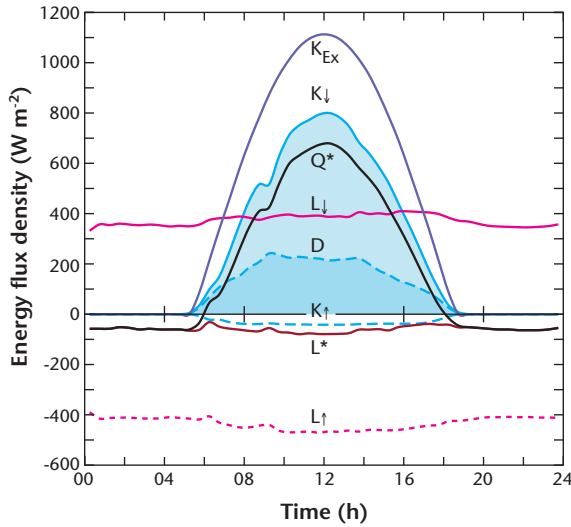
Figure 8: Variation of the radiation budget components for Lake Ontario near Grimsby, Ontario (43°N) on 28 August 1969, with cloudless skies (after Davies et al., 1970).

Longwave radiation from the atmosphere ($L_\downarrow$) is almost completely absorbed at a water surface with no significant reflection or transmission. The outgoing longwave flux ($L_\uparrow$) from a large water body is distinguished from that of most other natural surfaces by being virtually constant through the day. This is due to the very small diurnal range of surface water temperature.

Figure 8 presents results from one of the few studies over a water body in which almost all of the radiation budget components were measured. The observations were taken on an almost cloudless day, from a tower in Lake Ontario. The following general features emerge:

1. The extra-terrestrial solar input, K_{Ex} (computed not observed) describes a smooth symmetrical curve with a peak input at solar noon of slightly less than $1200\,\mathrm{W\,m^{-2}}$. This is less than the value of the solar constant ($1366.5\,\mathrm{W\,m^{-2}}$) because of the date and the latitude of the site. These factors determine that at solar noon the Sun is still $33.5°$ from the zenith (i.e. solar altitude = $56.5°$).

2. The surface receipt of shortwave ($K_\downarrow$) follows the same pattern as K_{Ex} but atmospheric attenuation (absorption, scattering and reflection) reduces the flux by about one-third. Of the receipt, 25 30% is as diffuse (D) and the remainder as direct-beam (S) (not plotted) at midday. This proportion increases to as high as 75% at lower solar altitudes due to the increased path length through the atmosphere.

3. The reflected shortwave radiation ($K_\uparrow$) is relatively small due to the very low albedo of water (daily average $\alpha = 0.07$, for diurnal variation at the same site see Figure 6). The diurnal course of the net short-wave radiation (K^*) is not plotted on Figure 7, but would obviously describe a curve equivalent to about 93% of $K_\downarrow$.

4. Both of the longwave fluxes are relatively constant with time due to the small diurnal temperature variation of lake surface and bulk air temperatures, respectively. Consequently the net longwave balance (L^*) shows an almost constant energy loss throughout the period.

5. The net allwave budget (Q^*) is dominated by K^* by day, and of course is equal to L^* at night. The daytime budget is notable for its high energy absorption values. At midday Q^* is almost $700\,\mathrm{W\,m^{-2}}$ due both to the low surface albedo (high K^*) and the relatively low surface temperature (low L^*).

In summary we may note that water surfaces are excellent absorbers of radiation, and that shortwave absorption occurs within a considerable volume. The convergence of the net radiative flux in the upper water layers leads to warming, but observed temperature variations are slight due to convection acting in the water as well.

Energy balance of water bodies. The energy balance of the surface layer of a water body (ocean, lake, pond or puddle) extending to a depth where there is no vertical heat transfer is given by:

$$Q^* = Q_H + Q_E + \Delta Q_S + \Delta Q_A \qquad \star \quad (8.10)$$

where ΔQ_S change of heat storage in the layer, ΔQ_A net horizontal heat transfer due to water currents. The schematic heat balance (Figure 9) shows that ΔQ_A is a form of horizontal heat flux convergence or divergence. If the water depth is small it is possible that net heat transfer by rainfall (Q_R) could be significant and should also be added to equation 8.10.

On an annual basis for large water bodies ΔQ_S can be assumed negligible (i.e. zero net heat storage). The energy balances of the major oceans are then as given in Table 3.1 which strikingly illustrates the dominant role played by evaporation (Q_E) as an energy sink for a water body. On an annual basis approximately 90% of Q^* is used to evaporate water, and this leads to characteristically small Bowen ratio (β) values of approximately 0.10.
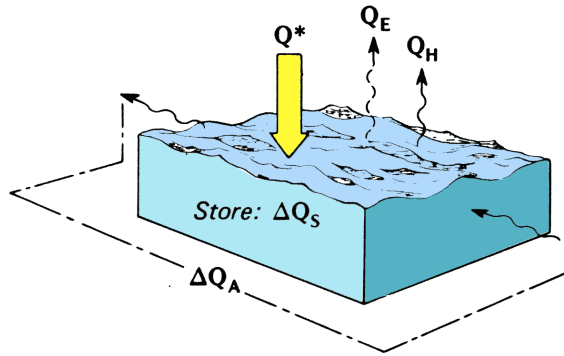
Figure 9: Schematic depiction of the fluxes involved in the energy balance of a water volume.

Radiation absorption by a water body is strong and it should be noted that for large portions of the daytime more of this energy is being used to heat the water (ΔQ_S). At night this energy store becomes the source of energy which sustains an upward flow of heat to the atmosphere throughout the period. Any water body therefore acts as a major heat sink by day, and a major heat source at night.

On a daily basis the complete energy balance (as per equation 8.10) can be obtained by including an estimated advective component (ΔQ_A) and a seasonal storage change (ΔQ_S). This leads to the situation where it is suggested that the buoyancy of air in the lowest layers over (mostly tropical) oceans is due more to their moisture, rather than their sensible heat content. This arises because the density of saturated air is less than that of dry air at the same temperature.

Differences from the those pattern of energy partitioning could arise as a result of localized advection by currents, or changes in air mass characteristics. A dry air mass enhances the evaporation rate (because the water-to-air humidity gradient is increased), and humid air suppresses it. Similarly the introduction of a relatively cold air mass enhances Q_H (because it causes the water-to-air temperature profile to become more lapse, and accordingly increases convective instability), whereas a warm one has a dampening effect. Phillips (1972) reports an example of enhanced Q_H over Lake Ontario in January. At this time the lake water is considerably warmer than the cold continental air traversing it. Climatological calculations show that Q_H may be as large as 20 MJ m^{-2} day^{-1} and since Q^* is very small at this time the energy output to the atmosphere must be derived from lake heat storage (ΔQ_S).

The thermal climate of water bodies. The thermal climate of a water body is remarkably conservative. This fact is clearly demonstrated by the water temperature profiles given in Figure 10. These observations are from a tropical ocean. A discernible diurnal heating/cooling cycle is evident but the maximum diurnal temperature range is only 0.275°C at the surface. On an annual basis the maximum range of sea surface temperature is 8°C at latitude 40°, and at the Equator it is only 2°C.

This presents a paradox; on the one hand, of all natural surfaces water bodies are noted to be about the best absorbers of radiation, but on the other, they exhibit very little thermal response. The lack of response can be attributed to four characteristics:

1. *penetration* since water allows shortwave radiation transmission to considerable depths energy absorption is diffused through a large volume;

2. *mixing* the existence of convection and mass transport by fluid motions also permits the heat gains/losses to be spread throughout a large volume;

3. *evaporation* unlimited water availability provides an efficient latent heat sink, and evaporative cooling tends to destabilize the surface layer and further enhance mixing (see below);

4. *heat capacity* the thermal capacity of water is exceptionally large such that it requires about three times as much heat to raise a unit volume of water through the same temperature interval as most soils.
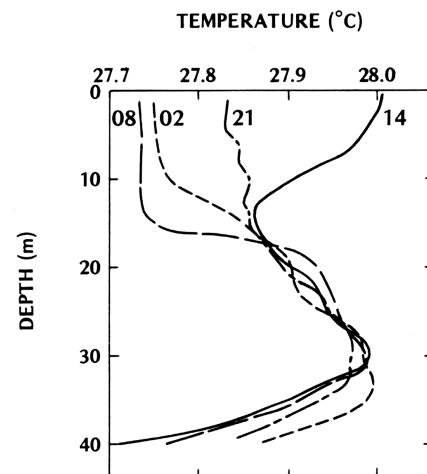

Figure 10: Diurnal sequence of ocean temperature profiles for the tropical Atlantic Ocean from measurements made in the period 20 June to 2 July 1969 (after Holland, 1971).

These four properties contrast with those of land surfaces. As noted previously, it is not uncommon to find surface temperature ranges of at least 20°C for soils, and this is almost two orders of magnitude greater than for water. Shorelines therefore demarcate sharp discontinuities in surface thermal climate, which in turn leads to horizontal cross-shoreline thermal gradients in the air and therefore pressure differences that induce breezes.

Figure 10 shows that the upper 30 m of the ocean is most active in diurnal heat exchange. Below this depth temperatures decrease rapidly. This zone is known as the thermocline and it divides the upper active mixed layer from the more stable layer beneath.

In lakes the upper layer is called the *epilimnion* and the lower one the *hypolimnion*. This division is important biologically because it tends to stratify habitats for thermally sensitive aquatic organisms. During the summer the epilimnion is warmer than the hypolimnion and species preferring cool water stay at depth. In cold winter climates the changeover occurs very rapidly due to the density characteristics of water. Pure water reaches its maximum density at about 4°C. In the spring, if the surface water temperature is below this value any warming serves to increase its density. Therefore warming of the surface leads to instability, the surface water sinks, and convective mixing raises the heat content of the upper layer relatively rapidly. After the surface has warmed beyond 4°C further warming only increases stability and restricts mixing (except by vigorous wave action) to the epilimnion. In the autumn, surface cooling again increases density, and therefore instability, and the epilimnion cools rapidly. It can also be seen that in the summer evaporative cooling of the surface destabilizes the upper layer so that over- turning brings warmer water to the surface and helps to maintain the almost constant temperature situation described above. This is an example of a negative feedback process.

In conclusion, it should be pointed out that much of the discussion has related to relatively large bodies of water (large lakes and oceans). In smaller systems (small lakes, ponds and puddles) the thermal inertia is reduced because of the smaller volume involved. For example, in a shallow water body the incoming shortwave radiation can penetrate to the floor. This warms the lower boundary of the system and the water is warmed from below as well as by the normal processes from above. If the water contains vegetation (e.g. reeds) this warming is further enhanced due to absorption by the submerged plants. Border-effects may also occur at the edges of a water body, and the smaller the width of the body the greater their influence. They arise because of heat conduction between the water body and the surrounding ground, and because of advection across the water margins (see Lecture 29).